AAC Accepts, published online ahead of print on 19 May 2014
Antimicrob. Agents Chemother. doi:10.1128/AAC.02994-14

Evaluation of SSYA10-001 as a Replication Inhibitor of SARS, MHV and MERS Coronaviruses

Adeyemi O. Adedeji[1,2,#], Kamalendra Singh[1,2], Ademola Kassim [1,2], Christopher M. Coleman[3], Ruth Elliott [4], Susan R. Weiss[4], Matthew B. Frieman[3] and Stefan G. Sarafianos[1,2,5,*]

[1]Christopher Bond Life Sciences Center, University of Missouri, Columbia, MO 65211; [2]Department of Molecular Microbiology & Immunology, University of Missouri School of Medicine, Columbia, MO 65211; [3]Department of Microbiology & Immunology, University of Maryland School of Medicine, Baltimore, MD 21201; [4]Department of Microbiology, University of Pennsylvania School of Medicine, Philadelphia, PA 19104; [5]Department of Biochemistry, University of Missouri, Columbia, MO 65211.

Running head: Specific inhibitor of SARS, MHV and MERS coronaviruses

* To whom correspondence should be addressed. Tel: +1-573-882-4338; Fax: +1-573-884-9676; Email: sarafianoss@missouri.edu

Present Address: Veterinary Medical Teaching Hospital, School of Veterinary Medicine, University of California, Davis, CA 95616

Abstract

We have previously shown that SSYA10-001 blocks Severe Acute Respiratory Syndrome Coronavirus (SARS-CoV) replication by inhibiting SARS-CoV helicase (nsp13). Here, we show that SSYA10-001 also inhibits replication of two other coronaviruses, Mouse Hepatitis Virus (MHV) and Middle Eastern Respiratory Syndrome Coronavirus (MERS-CoV). A putative binding pocket for SSYA10-001 was identified and shown to be similar in SARS-CoV, MERS-CoV and MHV helicases. These studies show that it is possible to target multiple coronaviruses through broad-spectrum inhibitors.

Findings

Coronaviruses are enveloped positive-sense RNA viruses that cause a range of diseases in humans and animals. The present study focuses on three highly pathogenic coronaviruses, two of which infect humans. Severe acute respiratory syndrome coronavirus (SARS-CoV) is responsible for the life-threatening viral respiratory illness known as SARS, which emerged from Southern China in November 2002 and spread to other parts of the world, including North America, South America, and Europe (1, 2). Middle East respiratory syndrome CoV (MERS-CoV) is a newly discovered coronavirus that caused severe pneumonia in patients in the Middle East (Saudi Arabia, Jordan, Qatar and the United Arab Emirates), Europe (UK, France, Italy, Germany) North Africa (Tunisia and Egypt) (3) and the United States of America. As of 5/13/2014, WHO lists 538 laboratory-confirmed cases of MERS-CoV infections worldwide, including 145 deaths (http://www.cdc.gov/media/releases/2014/p0512-US-MERS.html). Mouse hepatitis virus (MHV) is a murine coronavirus that can cause a wide range of illness in mice depending on the viral strain and the route of infection; these include respiratory, gastrointestinal, hepatic, and central nervous system (CNS) diseases (4). The MHV-A59 strain used in this study is a neuropathogenic strain. To date, there are no drugs approved for the treatment of any coronavirus infection.

We recently identified various small molecule inhibitors of SARS-CoV that target various steps of the SARS-CoV replication (5-8). Among them was SSYA10-001, a 1,2,4 triazole that prevents the helicase activity of SARS-CoV nsp13 and blocks SARS-CoV replication (8). We were particularly interested in this helicase inhibitor because unlike entry

inhibitors that target highly variable surface glycoprotein, SSYA10-001 targets the SARS-CoV nsp13 helicase, which shares significant homology with other coronavirus helicases (Figure 4). Hence, we hypothesized that the binding pocket of SSYA10-001 in SARS-CoV nsp13 is conserved among different coronavirus helicases, raising the exciting possibility of discovering broad-spectrum coronavirus inhibitors.

To locate the binding site of SSYA10-001 within SARS-CoV nsp13, we used three pocket-prediction programs: 'SiteMap' (Schrodinger Suite), 'SiteId' (Tripos Associates) and 'Q-site finder' (9). This approach identifies binding sites based on volumes roughly equivalent to the ligand volume, in this case SSYA10-001 (9). The putative binding site comprising residues Y277, R507 and K508 was chosen for further evaluation. We used site-directed amino-acid substitutions to construct SARS-CoV nsp13 enzymes with either of the following substitutions: Y277A, R507A, or K508A. Cloning and protein expression of these enzymes were as previously described (8). Two out of the three targeted proteins were successfully prepared to high homogeneity (>90%) and in active forms (Fig. 1A). We determined the unwinding activities of wild-type (WT), Y277A, and K508A SARS-CoV nsp13 helicases in the presence of varying concentrations of SSYA10-001 (0, 2.5, 5, 10, 25, 50, 75 and 100 μM), using a FRET-based assay as we previously described (8). The results showed that the Y277A and K508A amino-acid substitutions conferred resistance to SSYA10-001, as their estimated respective IC_{50} values were 12 and 50 μM respectively, compared to 5.9 μM for WT SARS-CoV nsp13 (Figure 1). Therefore, we concluded that Y277 and K508 are part of the binding pocket for SSYA10-001 within SARS-CoV nsp13. Importantly, sequence alignment of several coronavirus helicases revealed that the residues of the proposed inhibitor binding site are largely conserved in multiple coronaviruses (Figure 4). Hence, we built homology-derived molecular models of MERS-CoV, and MHV nsp13 helicases using 'Prime' software (for homology derived molecular models) and 'Glide' with extra precision (XP) and 'Induced Fit Docking' workflow (for docking), both integrated into 'Maestro' of Schrodinger Suite (Schrodinger Inc., NY) as previously described (10) . Comparison of the three modeled pockets revealed significant similarities (Figure 2) and suggested that SSYA10-001 may also be a potential antiviral for MHV and MERS-CoV.

To determine the effect of SSYA10-001 on MERS-CoV replication, VeroE6 cells were seeded into 96-well plates (Corning Costar) at $1x10^4$ cells per well and cultured overnight at 37°C. Cells were treated with SSYA10-001 at concentrations of 6.25 µM to 200 µM, or DMSO as a vehicle control, for 2 hours under normal culture conditions. MERS-CoV (Jordan strain) or SARS-CoV (MA15) was then added to each well at an MOI of 0.1. After 48 hours the supernatants were harvested. Viral load in the supernatants was assessed using a $TCID_{50}$ assay as previously described (7). Drug toxicity was assessed by incubating Vero E6 cells in the presence of SSYA10-001 for 48 hours and % cell survival was determined by using the CellTiterGlo® luminescent cell viability assay (Promega, Madison, WI) according to the manufacturer's instructions and read on a SpectraMax M5 plate reader (Molecular Devices, Sunnyvale, CA). As shown in Figure 3, SSYA10-001 inhibits MERS-CoV and SARS-CoV replications with EC_{50}s of ~ 25 µM (selectivity index = > 20), 7 µM (selectivity index = > 71) respectively as no significant cytotoxicity was observed even at 500 µM (Fig. 3D). To test the susceptibility of MHV-A59 to SSYA10-001, 4 X 10^4 mouse fibroblast L2 cells were seeded into each well in a 48-well plate. After 24 hrs, varying concentrations of SSYA10-001 (0, 10, 20, 40 and 80 µM) were added to the cells along with the MHV-A59 virus (R13) at an MOI of 0.01. After 24hrs, the cells were harvested and a standard plaque assay was performed to analyze the effect of the compound on MHV replication as previously described (11, 12). As shown in Figure 3C, SSYA10-001 inhibits MHV replication with an EC_{50} of ~12 µM.

Based on these results, SSYA10-001 is able to inhibit replication of at least three coronaviruses. Although, binding of SSYA10-001 has not been demonstrated in MERS-CoV and MHV nsp13, the molecular modeling data suggest that SSYA10-001 can be docked with comparable "Glide" score. Based on the similarities among the models of the inhibitor binding sites, we anticipate that other chemically related 1,2,4 triazoles could also bind to this conserved pocket and help the discovery of anti-coronavirus inhibitors. Ongoing studies are focused on *in silico* screening for the discovery of such inhibitors using the molecular models of these helicases.

In conclusion, we demonstrated through virological, biochemical, and molecular modeling studies that, SSYA10-001, a helicase targeting small molecule inhibitor of SARS-CoV helicase has antiviral effect against multiple coronaviruses by possibly targeting a

conserved binding pocket in nsp13. This compound could serve as a lead for the development of effective broad spectrum anti-coronavirus drugs.

Acknowledgements

This work was supported by the National Institutes of Health (AI076119, AI099284, AI100890, AI112417, and GM103368 to S. G. S. and AI079801 to M. A. P.). We also acknowledge support from Ministry of Knowledge and Economy, Bilateral International Collaborative R&D Program, Republic of Korea.

Figure Legends

Figure 1: Enzymatic activities of nsp13WT, nsp13 Y277A and nsp13 K508A in the presence and absence of SSYA10-001. (A) nsp13WT, nsp13 Y277A and nsp13 K508A (50 nM) were incubated in the presence of 20 mM HEPES, 20 mM NaCl, 0.01% BSA, 2 mM DTT, 5% glycerol, and 5 mM MgCl2. The helicase reaction was initiated by the addition of 100 nM 31/18-mer (13ss:18ds) as the substrate (Cy3 labeled) (8) at 30°C, along with 0.5 mM ATP and a 2 μM concentration of unlabeled ssDNA with a sequence complementary to that of the unlabeled DNA strand. The reactions were allowed to proceed for 10 min at 30°C, and the reaction was quenched with 100 mM EDTA, 0.2% SDS, and 20% glycerol. The products were separated and analyzed by 6% nondenaturing PAGE. (B) Helicase reactions for WT-nsp13 (Δ) and nsp13 Y277A (■) and nsp13 K508A (○) were performed in the presence of varying concentrations of SSYA10-001 inhibitor. The fraction of unwound DNA was plotted against the concentration of the inhibitor and the data was fit to a dose-response curve by GraphPad Prism 5.0. Experiments were performed in triplicates in three independent experiments, and error bars represent standard deviations for three independent experiments.

Figure 2: SSYA10-001 docking in inhibitor binding pockets of SARS-CoV, MERS-CoV, and MHV nsp13 helicase molecular models. Surface representation of molecular models of nsp13 helicases from three coronaviruses. The inhibitor binding sites with docked inhibitor molecules are shown for the three enzymes. The amino acid residues that are experimentally validated in the SARS-CoV enzyme and their equivalent residues in the other enzymes are shown as 'orange' surface area. The surface area for the rest of the molecules is shown by atom type (grey, carbon; red, oxygen; blue, nitrogen; yellow, sulfur). The equivalent residues in MERS-CoV and MHV helicases are also shown in orange surface area representation.

Figure 3: Effect of SSYA10-001 against (A) SARS-CoV, (B) MERS-CoV, (C) Mouse hepatitis virus (Neuropathogenic strain) and (D) Vero E6 cells. Virus titers or % cell viability are plotted against inhibitor concentrations using GraphPad Prism 5.0.

Experiments were performed in triplicates in three independent experiments and the and error bars represent standard deviations for three independent experiments.

Figure 4: Sequence alignment of nsp13/SF1 helicases from α, β and γ-coronaviruses. The dashes represent identical residues to SARS-CoV helicase. The stars represent the gap in the sequence. This figure shows six conserved SF1 helicase motifs, ATP hydrolysis active site (highlighted in red) in SARS-CoV (Accession #, AAP13442.1), HCOV-229E (Accession #, AAG48591.1), HCoV-HKU1 (Accession #, AAT98578.1), MHV (Accession #, NP_740617.1), MERS-CoV (Accession #, AFV09327.1), and TCoV (Turkey, Accession #, YP_001941186.1) nsp13s. SSYA10-001 binding pocket residues are highlighted in green. The first approximately N-terminal 240 residues are not shown for simplicity. The homology between SARS-CoV and 229E, NL63, HKU1, TCoV helicases is 76%, 76%, 82% and 68%, respectively.

REFERENCES

1) **Poutanen, S. M., D. E. Low, B. Henry, S. Finkelstein, D. Rose, K. Green, R. Tellier, R. Draker, D. Adachi, M. Ayers, A. K. Chan, D. M. Skowronski, I. Salit, A. E. Simor, A. S. Slutsky, P. W. Doyle, M. Krajden, M. Petric, R. C. Brunham, and A. J. McGeer.** 2003. Identification of severe acute respiratory syndrome in Canada. N Engl J Med **348:**1995-2005.
2) **Tsang, K. W., P. L. Ho, G. C. Ooi, W. K. Yee, T. Wang, M. Chan-Yeung, W. K. Lam, W. H. Seto, L. Y. Yam, T. M. Cheung, P. C. Wong, B. Lam, M. S. Ip, J. Chan, K. Y. Yuen, and K. N. Lai.** 2003. A cluster of cases of severe acute respiratory syndrome in Hong Kong. N Engl J Med **348:**1977-1985.
3) **Raj, V. S., H. Mou, S. L. Smits, D. H. Dekkers, M. A. Muller, R. Dijkman, D. Muth, J. A. Demmers, A. Zaki, R. A. Fouchier, V. Thiel, C. Drosten, P. J. Rottier, A. D. Osterhaus, B. J. Bosch, and B. L. Haagmans.** 2013. Dipeptidyl peptidase 4 is a functional receptor for the emerging human coronavirus-EMC. Nature **495:**251-254.
4) **Cowley, T. J., and S. R. Weiss.** 2010. Murine coronavirus neuropathogenesis: determinants of virulence. J Neurovirol **16:**427-434.
5) **Adedeji, A. O., B. Marchand, A. J. Te Velthuis, E. J. Snijder, S. Weiss, R. L. Eoff, K. Singh, and S. G. Sarafianos.** 2012. Mechanism of nucleic acid unwinding by SARS-CoV helicase. PLoS One **7:**e36521.
6) **Adedeji, A. O., and S. G. Sarafianos.** 2013. Future treatment strategies for novel Middle East respiratory syndrome coronavirus infection. Future Med Chem **5:**2119-2122.
7) **Adedeji, A. O., W. Severson, C. Jonsson, K. Singh, S. R. Weiss, and S. G. Sarafianos.** 2013. Novel inhibitors of severe acute respiratory syndrome coronavirus entry that act by three distinct mechanisms. J Virol **87:**8017-8028.
8) **Adedeji, A. O., K. Singh, N. E. Calcaterra, M. L. DeDiego, L. Enjuanes, S. Weiss, and S. G. Sarafianos.** 2012. Severe acute respiratory syndrome coronavirus replication inhibitor that interferes with the nucleic acid unwinding of the viral helicase. Antimicrob Agents Chemother **56:**4718-4728.
9) **Laurie, A. T., and R. M. Jackson.** 2005. Q-SiteFinder: an energy-based method for the prediction of protein-ligand binding sites. Bioinformatics **21:**1908-1916.
10) **Adedeji, A. O., K. Singh, and S. G. Sarafianos.** 2012. Structural and biochemical basis for the difference in the helicase activity of two different constructs of SARS-CoV helicase. Cell Mol Biol (Noisy-le-grand) **58**:114-21.
11) **Gombold, J. L., S. T. Hingley, and S. R. Weiss.** 1993. Fusion-defective mutants of mouse hepatitis virus A59 contain a mutation in the spike protein cleavage signal. J Virol **67:**4504-4512.
12) **Zhao, L., L. D. Birdwell, A. Wu, R. Elliott, K. M. Rose, J. M. Phillips, Y. Li, J. Grinspan, R. H. Silverman, and S. R. Weiss.** 2013. Cell-Type-Specific Activation of the Oligoadenylate Synthetase-RNase L Pathway by a Murine Coronavirus. J Virol **87:**8408-8418.

219

220

221

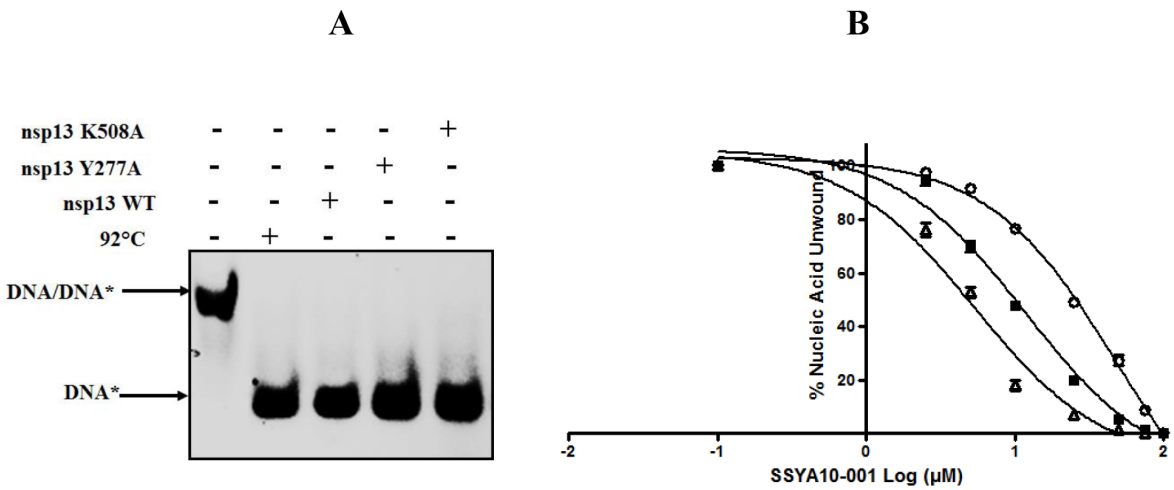

Figure 1

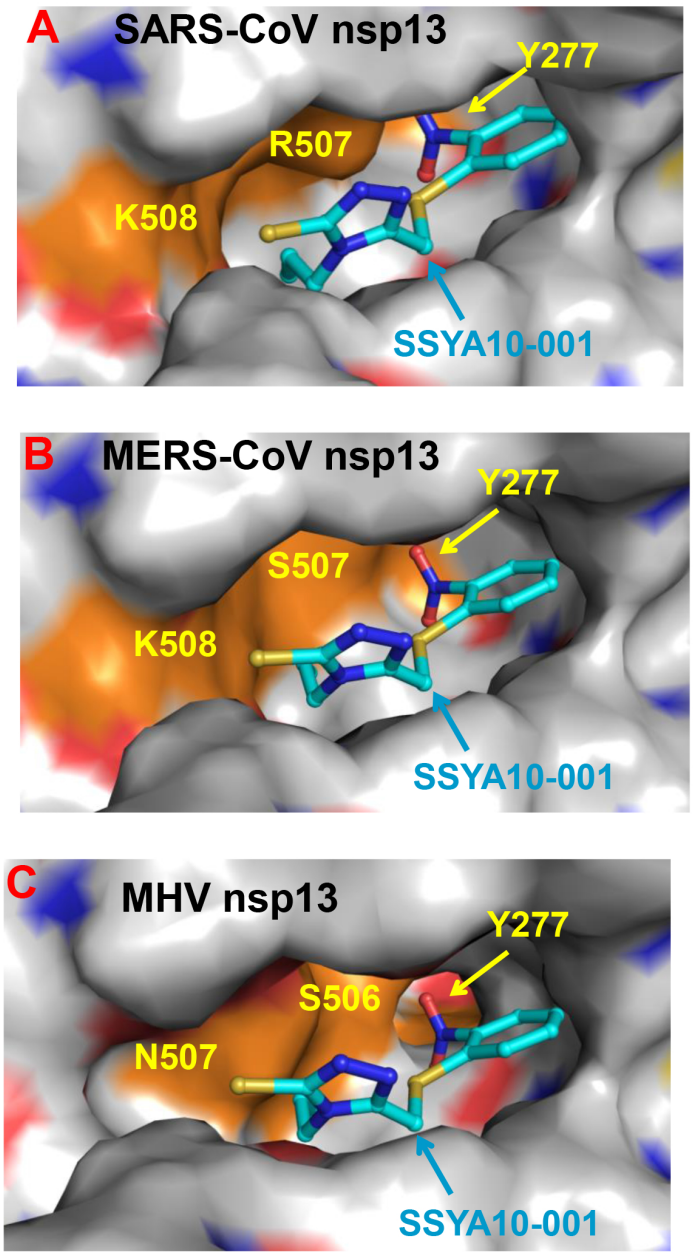

Figure 2

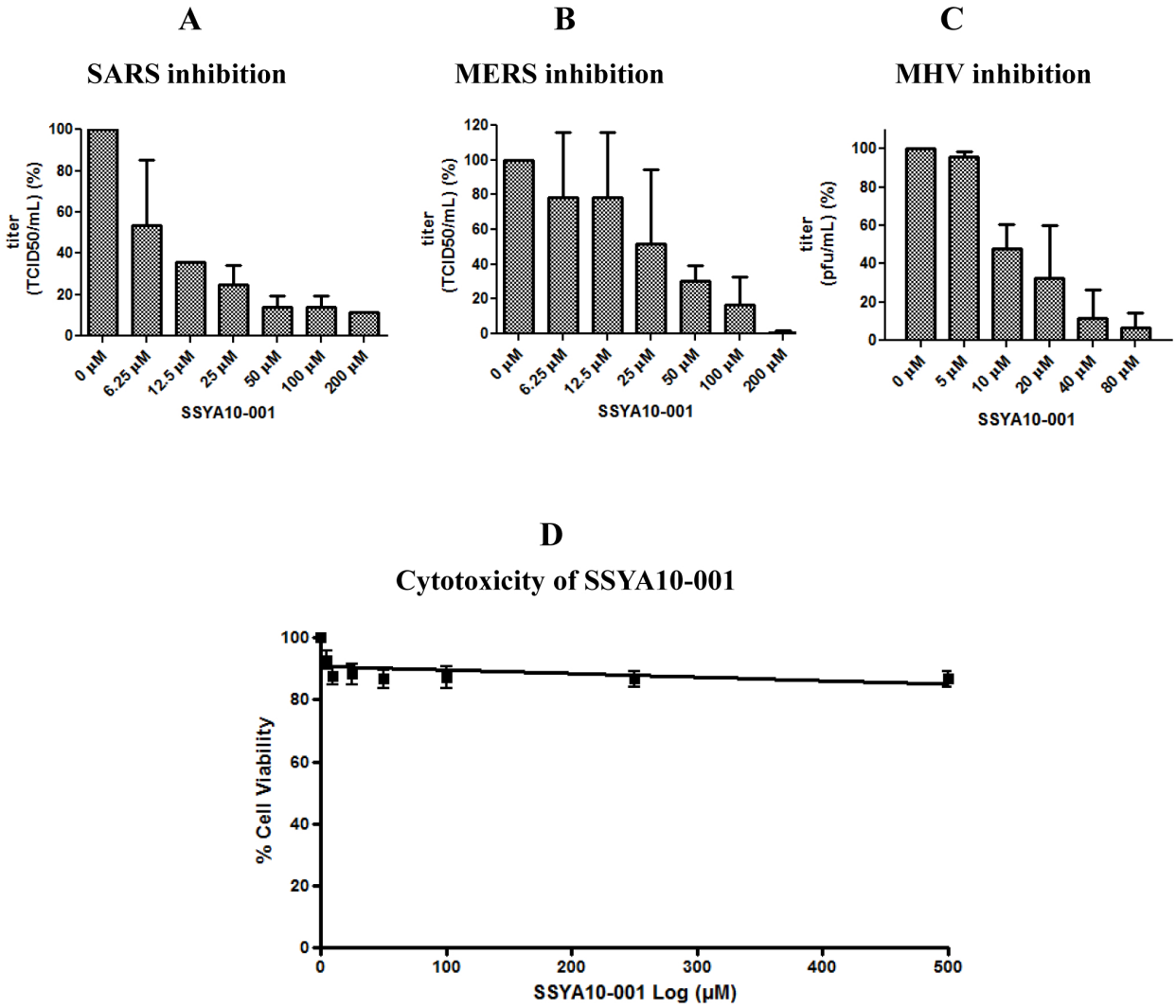

Figure 3

.

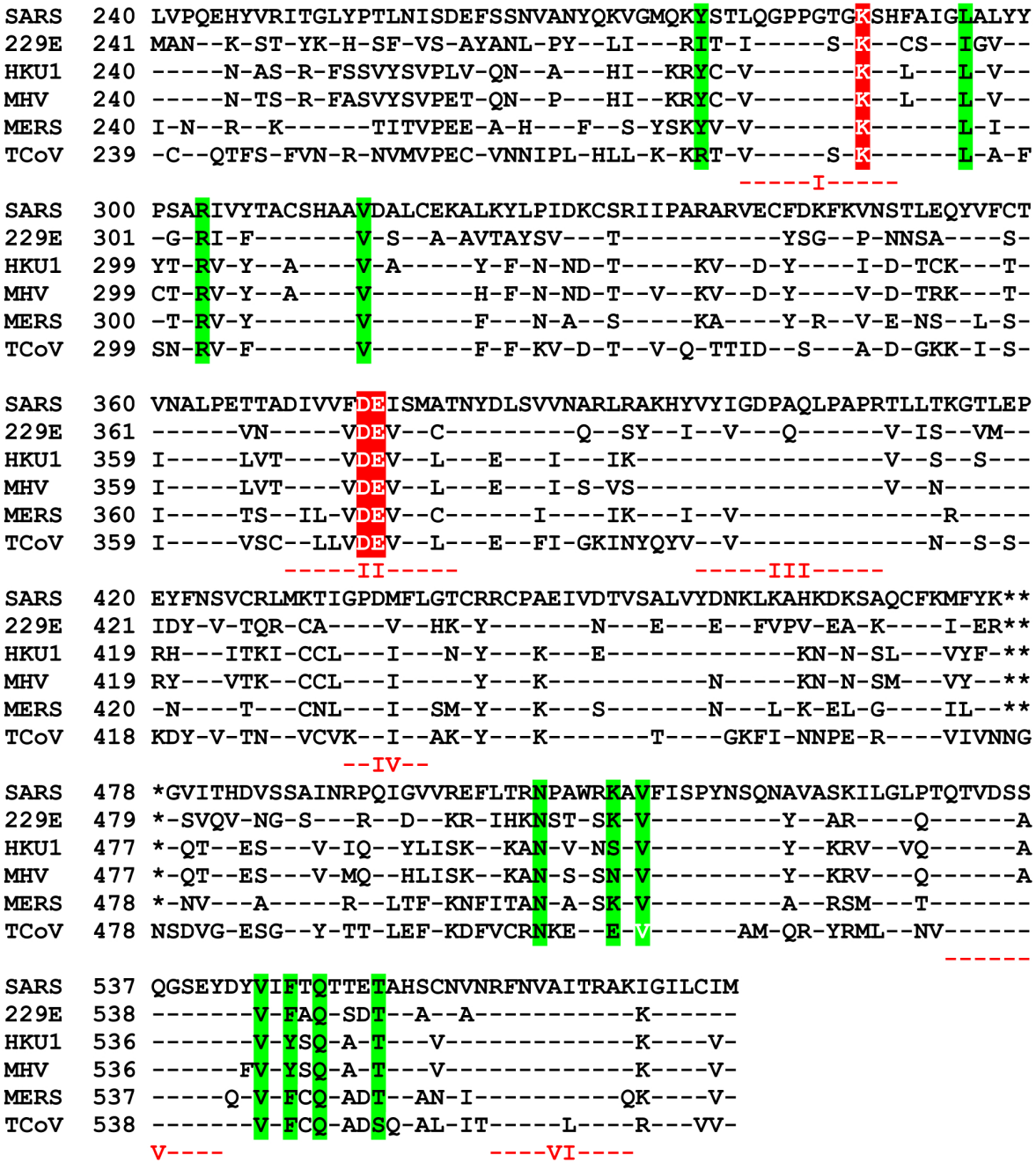

Figure 4